Multi-band Measurements for Deep Learning-based Dynamic Channel Prediction and Simulation

Faruk Pasic*, Nicola Di Cicco†, Marco Skocaj‡, Massimo Tornatore†, Stefan Schwarz*,
Christoph F. Mecklenbräuker* and Vittorio Degli-Esposti‡
*Institute of Telecommunications, TU Wien, Austria
†DEIB, Politecnico di Milano, Italy
‡DEI, University of Bologna, & WiLab, CNIT, Italy
faruk.pasic@tuwien.ac.at, nicola.dicicco@polimi.it

***Abstract*—Next-generation mobile communication systems are planned to support millimeter Wave (mmWave) transmission in scenarios with high-mobility, such as in private industrial networks. To cope with propagation environments with unprecedented challenges, data-driven methodologies such as Machine Learning (ML) are expected to act as a fundamental tool for decision support in future mobile systems. However, high-quality measurement datasets need to be made available to the research community in order to develop and benchmark ML-based methodologies for next-generation wireless networks. We present a reliable testbed for collecting channel measurements at sub-6 GHz and mmWave frequencies. Further, we describe a rich dataset collected using the presented testbed. Our public dataset enables the development and testing of innovative ML-based channel simulators for both sub-6 GHz and mmWave bands on real-world data. We conclude this paper by discussing promising experimental results on two illustrative ML tasks leveraging on our dataset, namely, channel impulse response forecasting and synthetic channel transfer function generation, upon which we propose future exploratory research directions. The original dataset employed in this work is available on IEEE DataPort[1], and the code utilized in our numerical experiments is publicly accessible via CodeOcean[2]**

***Index Terms*—machine learning, deep learning, radio channel prediction, radio channel simulation, vehicular communications, channel sounding, channel measurements.**

I. Introduction

Adaptive wireless transmission is among the core paradigms for achieving consistent communication performance close to the Shannon limit [2]. In particular, to estimate the quality of a radio link and to adapt the transmission parameters to the current channel condition, the transmitter needs to know the Channel State Information at the Transmitter (CSIT), i.e., a set of channel properties of the radio link. These properties are strongly affected by several propagation phenomena such as path loss, scattering, fading and shadowing [3]. Accurate CSIT knowledge allows optimally tuning several transmission parameters e.g., the transmit power, constellation size, coding rate, single- and multiuser-beamforming/precoding, as well as scheduling and resource allocation. Whenever link adaptation is based on the assumption of instantaneous CSIT, outdated CSIT can cause significant performance degradation [4]. For example, feedback delay and processing delay in frequency-division duplex (FDD) and time-division duplex (TDD) systems, respectively, are causes of outdated CSIT. Both feedback and processing delays become more severe in rapidly changing fading channels.

To deal with the problem of outdated CSIT in a data-driven way, researchers have already proposed several channel prediction methods based on ML. The goal of channel prediction is to accurately forecast future CSIT in advance with a time span that counteracts the induced delay. The proposed methods are mostly based on Recurrent Neural Networks (RNN), as they are especially suited for processing time-series data [5]. For example, in [6], authors develop a channel forecaster based on Long Short-Term Memory (LSTM) and Gated Recurrent Unit (GRU) neural network layers.

In this context, next-generation mobile communication systems are planned to support mmWave transmission and are expected to operate in high-mobility scenarios. 5G private industrial networks, for instance, are planned to operate indoors at sub-6 GHz and mmWave frequencies. High mobility, in this case, often refers to rapidly moving and rotating parts of industrial machines. Motion control and Mobile Control Panels - two of the interest use cases suggested by the 5G Alliance for Connected Industries and Automation (ACIA) - are systems in charge of accurately controlling, maintaining and detecting faults of these moving parts with a closed control loop involving the periodical collection of data from built-in transmitting sensors. In this scenario, the co-location of antennas and sensors on mobile parts is imperative for continuously monitoring their proper functionality in a timely manner. Due to fast channel fading, abrupt shadowing transitions and larger Doppler spreads, channel prediction in the scenario introduced above poses a significant challenge. Hence, high-quality datasets of channel measurements in high-speed scenarios are required for benchmarking ML-based techniques in real-world conditions.

However, collecting reliable and self-consistent datasets of comparative measurements between sub-6 GHz and mmWave bands is not trivial. For instance, sub-6 GHz and mmWave antennas cannot be simultaneously mounted at exactly the same physical location. Such an antenna displacement may result in a different fading behavior for different frequency

F. Pasic and N. Di Cicco are co-first authors of this paper.
[1]Link to IEEE DataPort dataset: [1] https://dx.doi.org/10.21227/3tpp-j394
[2]Link to CodeOcean: https://codeocean.com/capsule/9619772/tree

bands, thus altering a fair comparison.

In this paper, to address these multifaceted challenges, we provide the research community with a reliable and rich high-speed channel measurements dataset for both sub-6 GHz and mmWave frequencies, and we illustrate its potential application for ML-based channel forecasting and simulation. The testbed introduced in this study emulates the typical motion patterns exhibited by mechanical components in industrial machines, and is therefore of particular interest for the characterization of sub-6 GHz and mmWave 5G industrial communications scenarios. Our contributions are summarized as follows:

- We present the testbed hardware (published in [7]) for fairly comparing systems between different frequency bands in terms of small-scale and fast-fading in a high-mobility environment.
- We describe a methodology (published in [8]) that allows multi-band channel sounding over the identical measured antenna path.
- We describe our dataset of channel measurements at sub-6 GHz and mmWave bands, with transmitter velocities of 40 km/h and 100 km/h.
- We present two illustrative use cases of our dataset for the application of ML-based techniques: RNN-based channel forecasting and Generative Adversarial Network-based channel impulse response (CIR) simulation.

II. Testbed Design and Implementation

This section presents the proposed testbed setup. We focus on the testbed implementation for sub-6 GHz and mmWave cases, as well as on the necessary time and frequency synchronization. We then elaborate on the two major advantages of the proposed testbed: reproducibility and controllability. Finally, we introduce a methodology for comparing multi-band measurements performed at different transmitter velocities in a fair manner.

A. Testbed Hardware

Our testbed setup is composed of a moving transmitter and a static receiver, both located in an indoor propagation environment [8]. Our moving transmitter employs a rotary unit [9] which spins a transmit antenna around a central axis. Specifically, the transmit antenna is placed on the top of a 1 m long, rotating aluminum alloy arm that can reach speeds up to 400 km/h, i.e., up to 1000 rotations-per-minute (rpm). We control the rotation speed using an frequency inverter.

Furthermore, the rotary unit includes two rotary joints at both ends of the central axis. The rotary joints are used to connect the two rotating coaxial cables inside the rotary arm to the static cables and the signal source outside the arm. The maximum allowed signal frequency for these rotary joints is 12.4 GHz. Thus, while sub-6 GHz signals can be directly transmitted to the arm end, mmWave signals cannot. To the best of our knowledge, a rotary joint capable of both mmWave transmission and rotation up to approximately 1000 rpm is not available off-the-shelf. Therefore, the testbed setup requires hardware modifications to enable mmWave transmission.

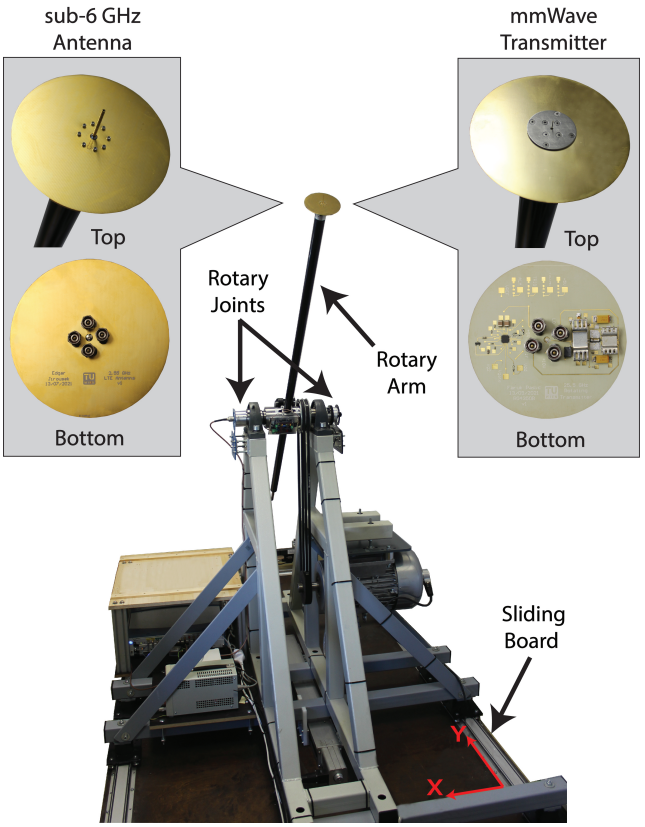

Fig. 1. Testbed setup for multi-band time-variant channel measurements. A transmit antenna is attached at the edge of the rotating arm.

In the following, for both sub-6 GHz and mmWave cases, we generate the signal with an Arbitrary Waveform Generator (AWG) (Keysight M8195A) and sample the received signal with a signal analyzer (Rohde & Schwarz FSW67).

B. Sub-6 GHz Setup

The transmit Intermediate Frequency (IF) signal is digitally up-converted via the AWG to the 2.55 GHz center frequency. Then, the up-converted signal is transmitted through the rotary joint and the coaxial cable up to the end of the rotary arm. Finally, the radio signal is transmitted by a monopole antenna shown in Fig. 1.

C. Millimeter Wave Setup

In the mmWave case, as previously mentioned, a direct transmission of the Radio Frequency (RF) signal through the rotary joint is not possible. Thus, we mount a mmWave transmitter at the edge of the rotary arm and perform frequency up-conversion. Since the edge of the rotary arm is exposed to non-negligible acceleration forces during rotation, using off-the-shelf, bulky RF modules is unfeasible. As a possible solution, we developed our mmWave transmitter on a 6-layered Printed Circuit Board (PCB) with the RF dielectric substrate Rogers RO4350B (see Fig. 1). The PCB consists of Surface Mount Device (SMD) components on the bottom side and a monopole antenna on the top side. The entire PCB is remarkably lightweight, weighing only 43.1 grams.

As before, the IF signal is up-converted to the center frequency of 5.5 GHz by the AWG. In addition, the mmWave transmitter uses a Local Oscillator (LO) signal to up-convert the signal to RF domain. Specifically, the LO signal at the center frequency of 10 GHz is generated with a Continuous Wave (CW) signal generator (R&S SMF). The IF and LO signals are transmitted through the two rotary joints to the mmWave transmitter, which is placed at the edge of the rotating arm.

Besides the IF and LO signals, the mmWave transmitter requires a $+5$ V and a $+10.175$ V DC supply. In our setup, as the two rotary joints are being used for high-frequency signals, we mounted a battery on the central rotating axis. In this way, the DC supply is exposed only to negligible acceleration forces.

Within the mmWave transmitter, an up-converter Integrated Circuit (IC) performs LO frequency doubling. The doubled LO frequency mixed with the IF signal leads to an RF frequency of 25.5 GHz. As the up-converter, we use the Macom MAMF-011024, which operates in the frequency range from 21 to 27 GHz. Undesired spectral components (e.g., higher-order harmonics, intermodulation products) generated by the up-converter are filtered out via a $25-26$ GHz bandpass filter (B259MC1S). Furthermore, we leverage on a power amplifier (HMC994APM5E) for compensating the large path losses at mmWave frequencies. Finally, the amplified mmWave signal is radiated by a 25.5 GHz monopole antenna.

For fairly comparing sub-6 GHz and mmWave frequency bands, we require the same receive antenna raditation patterns for both scenarios. Therefore, we employ 2.55 GHz and 25.5 GHz horn antennas with the same opening angle as receive antennas for sub-6 GHz and mmWave, respectively.

D. Synchronization

To reach optimum performance of the proposed channel sounding system, accurate frequency and timing synchronization are required. For instance, in a typical Industrial Internet of Things (IIoT) scenario, multiple transmitter devices are often located on moving mechanical parts and far away from each other. Hence, a cable connection for providing precise frequency and timing synchronization between sensing devices and the receiver is not feasible. Instead, to provide precise frequency synchronization, expensive Rubidium frequency standards are usually employed at the transmitter and the receiver [10]. As a possible solution for precise timing synchronization, a preamble with good auto-correlation properties is often exploited to detect the starting point of the signal at the receiver [11].

In our setup, the transmitter and the receiver are placed only 10 m apart in the indoor laboratory environment. Therefore, the cable connection is feasible and it represents a significant advantage of the proposed setup compared to usual ones. To provide accurate frequency synchronization, we interconnect the AWG at the transmitter's site and the signal analyzer at the receiver's site with a 100 MHz reference. For time synchronization, we equip the rotary unit with a triggering unit based on a Field Programmable Gate Array (FPGA) and a rotational encoder. A trigger signal is derived by decoding the signal of the rotational encoder via a counter and a comparator. The generated trigger signal is fed to both the transmitter and the receiver. Therefore, measurements can be initiated at a specific and previously defined angular position of the rotating arm once per revolution.

E. Reproducibility and Controllability

Two major advantages of the proposed testbed setup are reproducibility and controllability. Reproducibility is the ability to replicate a sample under identical channel conditions, which can hardly be achieved in real-world measurements. For instance, in industrial communication scenarios, it is extremely unlikely that the surroundings of a machine being monitored (e.g., other machines and human operators) remain constant over time. Our testbed setup achieves reproducibility in the following way.

Firstly, the fading environment is kept static by ensuring that there are no moving obstacles in the measurement room during the experiment. This enables us to observe the effect of individual system parameters (e.g., velocity, transmit power). Secondly, via the trigger unit, we ensure that the transmit antenna moves over an identical circular trace at the same constant velocity for both sub-6 GHz and mmWave frequencies. Thirdly, the receive antenna is kept static for the whole duration of the measurement campaign. Therefore, we are able to fairly compare measurements at sub-6 GHz and mmWave frequencies.

The second major advantage of our proposed setup is controllability, which is the ability to control environmental and system parameters. Indeed, our setup allows fine tuning of individual parameters of the radio link. For instance, we can easily change the receive power by adjusting the transmit power, and control the transmitter velocity by adjusting the rotation speed through the frequency inverter.

F. Ensuring Fair Comparisons

To fairly compare measurements performed at various velocities and frequency bands, we extend the methodology from [8]. Firstly, the fading environment is kept static. To this end, we ensured that there are no moving obstacles in the measurement room during our experiments. Secondly, we dimension the symbol duration such that the same number of symbols is transmitted along the same measured trace for different velocities. Overall, our parameter selection makes the measurement results independent of the transmitter's velocity, and therefore leads to a fair comparison.

III. Dataset

In this section, we first describe our measurement campaign with all measured scenarios and explain the post-processing procedure of the measurement results to obtain our dataset. Subsequently, we show some examples of data extraction and provide practical guidelines for using our dataset.

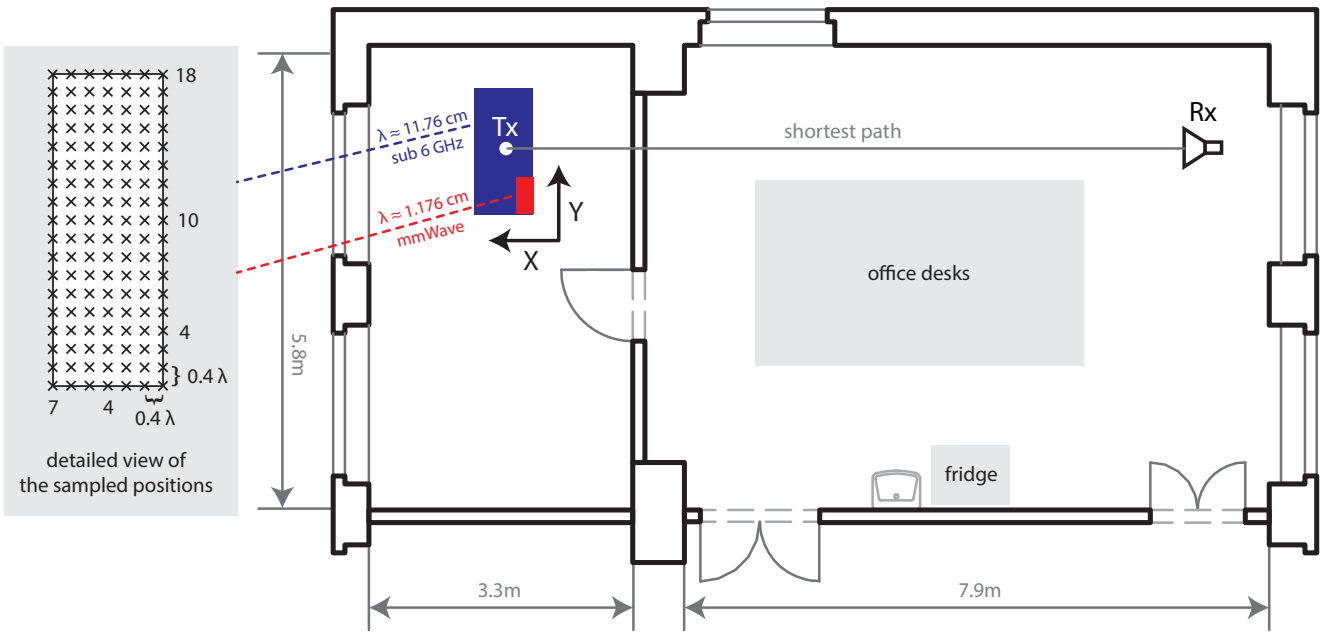

Fig. 2. Measured indoor laboratory environment. The rotating transmitter and the statical receiver are located in adjacent rooms. The transmitter is placed on a sliding board, which is moved according to the illustrated rectangular grid.

A. Measurement Campaign

Using the above described testbed and methodology, we perform channel measurements in the indoor propagation environment illustrated in Fig. 2. Since indoor Line-of-Sight (LOS) scenarios have already been well investigated, we focused on a more challenging indoor Non-Line-of-Sight (NLOS) scenario, which is more representative of real-world IIoT scenarios. We perform channel measurements in four scenarios at the center frequency of 2.55 GHz or 25.5 GHz, and transmitter velocity of 40 km/h or 100 km/h. The detailed list of channel sounding parameters is reported in Tab. I. The moving transmit antenna follows the same circular arc segment at a constant velocity. The receive antenna is kept static, being placed on a table in an adjacent room.

We employ an Orthogonal Frequency-Division Multiplexing (OFDM) Zadoff-Chu sequence [12] as the channel-sounding signal. Specifically, a single measurement sequence consists of 50 000 identical OFDM symbols. Each measurement sequence is grouped into 500 snapshots, and each snapshot consists of 100 OFDM symbols. Here, we assume that the coherence time of the measured channel is larger than the duration of one snapshot. The trigger unit starts the transmission when the rotary arm is at a position of $-40°$. The transmission continues as the antenna moves along the circular arc from $-40°$ to $40°$, corresponding to a trace length of 1.39 m. Note that the angular position of $0°$ corresponds to the direction perpendicular to the ceiling.

At the receiver, the first OFDM symbol of each snapshot is used as a cyclic prefix to remove intersymbol interference (ISI), and the remaining 99 symbols are averaged, thereby improving the Signal-to-Noise Ratio (SNR) by roughly 20 dB. Once the OFDM signal processing is completed, the wireless channel for each subcarrier is estimated via least-squares. We therefore obtain doubly-selective channel transfer functions.

TABLE I
CHANNEL SOUNDING PARAMETERS

Parameter	Value			
Bandwidth [MHz]	100			
Number of Snapshots	500			
Symbols per Snapshot	100			
Delay Resolution [ns]	10			
x-axis Positions	7			
y-axis Positions	18			
Measured Arc Segment	$-40° \ldots 40°$			
	A	**B**	**C**	**D**
Carrier Frequency [GHz]	2.55	2.55	25.5	25.5
Tx Velocity [km/h]	40	100	40	100
Number of Subcarriers	250	100	250	100
Subcarrier Spacing [kHz]	400	1000	400	1000
Symbol Duration [µs]	2.5	1	2.5	1
Measurement Duration [ms]	125	50	125	50
Maximum Doppler Shift [Hz]	94.5	236.2	945	2362

Using this measurement procedure, we generate a dataset consisting of different doubly-selective channel transfer functions. These functions are generated by conducting measurements at different positions of the transmitter. Besides rotating, we can move the transmitter in space as well. Specifically, the rotary unit with the transmit antenna is mounted on a sliding board, which can be moved in space. We assume local stationarity of the doubly-selective channel within a window of approximately six wavelengths. At center frequencies of 2.55 GHz and 25.5 GHz, six wavelengths correspond roughly to 70 cm and 0.7 cm, respectively. Under the aforementioned assumptions, we performed measurements at 126 different

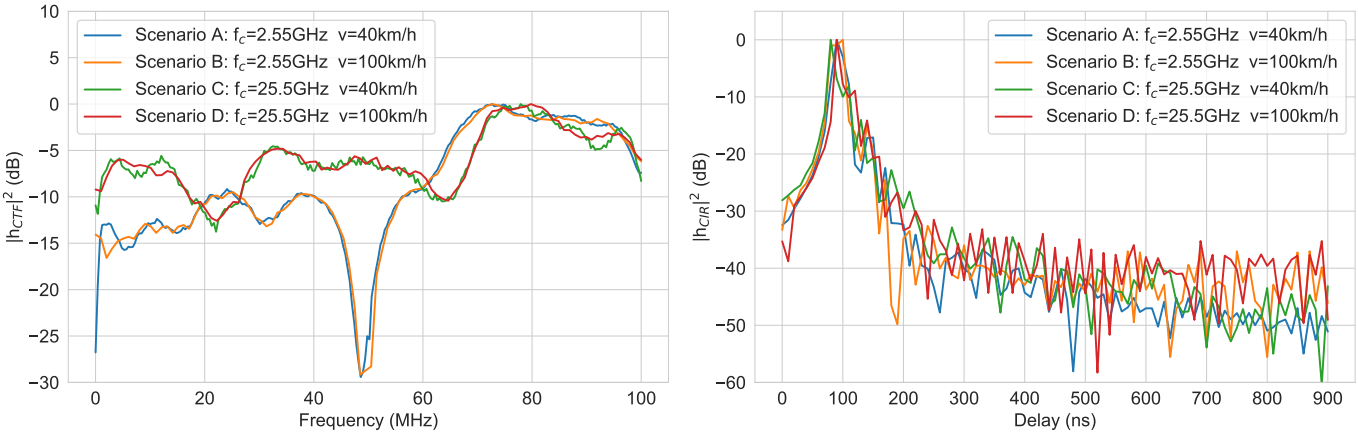

Fig. 3. Channel transfer function and channel impulse response of the 50th snapshot in all of the measured scenarios. Location on the x-y axis is X0Y0.

positions, as illustrated in Fig. 2. The positions on the x- and y-axis are mutually separated by 0.4 λ. The blue (large) and red (small) rectangles indicate the measured region for sub-6 GHz and mmWave, respectively. Thereby, we obtain different realizations of the same wireless channel for both sub-6 GHz and mmWave.

B. Dataset Description

The dataset is accessible via IEEE DataPort [1], and consists of doubly-selective channel transfer functions classified in four categories depending on the measurement scenarios in Tab. I. Our dataset is provided as numpy (.npy) files. Each .npy file contains a 2D complex-valued matrix, where rows represent snapshots and columns represent subcarriers. For each scenario, there are 126 channel realizations obtained by conducting measurements at different positions in accordance with the grid from Fig. 2. Each filename in the dataset is formatted as "frequency_velocity_position". For example, the entry "25_5GHz_100kmh_X6Y2.npy" denotes the doubly-selective channel transfer function measured at 25.5 GHz at the velocity of 100 km/h for the position six on the x-axis and position two on the y-axis.

Additionally, we provide an illustrative "example.py" script for visualizing our dataset. The script loads measurement samples according to user-specified parameters, such as the x- and y- positions within the rectangular grid, and displays the measured channel transfer function (CTF) and the channel impulse response (CIR). Specifically, the script computes the CIR via Inverse Fast Fourier Transform (IFFT) of the corresponding CTF. As an illustrative example, in Fig. 3, we show the CTF and CIR for the 50^{th} snapshot and positions X0Y0 for all measured scenarios.

IV. Illustrative Machine Learning Use-Cases and Exploratory Research Directions

In this Section, we outline two illustrative ML use-cases for the presented dataset, namely i) CIR forecasting using recurrent neural networks, and ii) CTF simulation using generative neural networks. For each task we describe a baseline ML approach, we discuss our main results, and we propose future research directions.

A. Channel Forecasting with Recurrent Neural Networks

We consider the problem of forecasting CIR values over a fixed time horizon, given a time-series of past CIR values. In the context of an adaptive transmission systems, accurate CIR forecasting can help mitigating the problem of outdated CSIT in the presence of fast fading [6].

To implement our forecaster, we leverage Long Short Term Memory (LSTM) neural networks with Variational Dropout. LSTM networks can efficiently learn complex temporal dependencies in the sequence of input CIR values. Variational Dropout allows to estimate the uncertainty associated with each forecast, providing richer information for proactive decision-making compared to single point-estimates.

Our channel forecaster is implemented as a classical encoder-decoder architecture, which comprises an encoder neural network and a decoder neural network. More specifically, the encoder and decoder networks consist of multiple LSTM layers with Variational Dropout [13]. The task of the encoder is to produce a fixed-dimension vector (often referred to as context vector) from an input time-series of past CIR values. The decoder takes as an input the context vector and the last (either ground-truth or forecasted) CIR value, and outputs a forecast for the CIR value at the next time instant as well as an updated context vector. The forecasted CIR value and the updated context vector are auto-regressively fed back to the decoder, and the process is repeated until the desidered forecast time-horizon is reached.

As an illustrative task, we will consider forecasting the absolute CIR values for a single subcarrier, i.e., we limit ourselves to a simple univariate forecasting problem. In particular, we train our neural network to predict the future 32 CIR snapshots given 64 past CIR snapshots.

Fig. 4 shows an illustrative CIR forecast for 2.55GHz center frequency and 40km/h speed. Our encoder-decoder model correctly captured the CIR time-varying behaviour and it is able to produce accurate forecasts. In particular, the ground-truth CIR values are almost always within the predicted 95% confidence

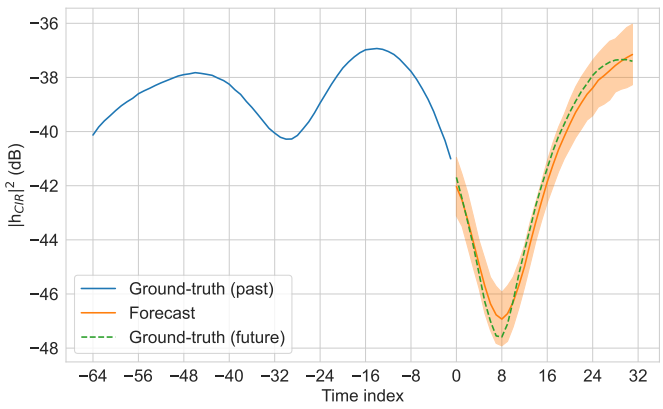

Fig. 4. Illustrative CIR mean forecasts and 95% confidence bands for a single OFDM subcarrier, 2.55 GHz center frequency and 40 km/h transmit antenna speed.

bands, therefore providing a truthful interval in which the ground-truth CIR values are expected to lie. As expected, due to forecasting errors compounding over time, the CIR forecasts become increasingly inaccurate as the forecasting horizon grows. On average, over all the considered measurement points in the room, the Mean Absolute Percentage Error (MAPE) of the forecasts is approximately $9.3 \pm 0.2\%$, which indicates good overall forecasting performance.

As exploratory future reseach, joint forecasting of multiple subcarriers can be investigated. In particular, leveraging on state-of-the-art attentional models [14], temporal correlations between different subcarriers can be exploited for producing more accurate forecasts, and for quantitatively evaluating the impact of each subcarrier in the output forecasts.

B. Channel Simulation with Generative Neural Networks

We consider the problem of building an approximate and lightweight channel simulator from channel sounding measurement data. More specifically, we aim at generating synthetic CTF samples whose behaviour over frequency and time mimics real-world measurements. Illustrative applications include the design of radio interfaces and systems in propagation environments similar to the training data, and benchmarking transmission and coding techniques in realistic, but diversified stochastic channel samples.

We propose leveraging generative neural networks for building approximate channel simulators. Briefly, the learning objective of generative neural networks is to model the distribution of a given dataset (in our case, CTF samples). Said distribution can then be cheaply sampled from, allowing for cheap generation of arbitrarily large volumes of new, synthetic data.

Leveraging on recent advances in synthetic generation of image data, we implement our generative network as a Deep Convolutional Generative Adversarial Network (DCGAN) [15]. In particular, we consider the task of generating synthetic samples of the absolute CTF value over time and frequency. As such, we represent each experimental run in our presented dataset as a single image. At full resolution, each

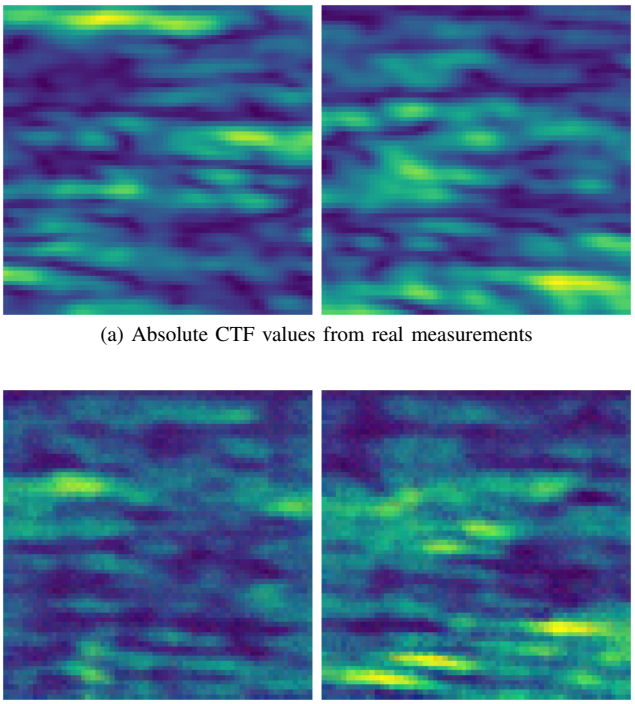

(a) Absolute CTF values from real measurements

(b) Absolute CTF measurements generated by a DCGAN

Fig. 5. Illustrative real and synthetic absolute CTF values for 2.55 GHz center frequency and 40 km/h transmit antenna speed. Time/frequency are the horizontal/vertical axes.

image will have height equal to the number of OFDM carriers, and width equal to the number of samples. For keeping training times reasonably short and facilitating convergence, we resize our input data down to 64x64.

Fig. 5 illustrates real and synthetic absolute CTF values for a center frequency of 2.55GHz and velocity equal to 40km/h. The synthetic CTF samples, albeit looking slightly noisy, are indeed visually resemblant to the real measurements. We underline that by leveraging off-the-shelf Graphical Processing Units (GPUs), large volumes of synthetic data can be generated in short computational times. Thus, our simple exercise illustrates the potential of generative neural networks for building realistic channel simulators.

V. Conclusion

In this paper, we describe the testbed hardware for collecting comparative doubly-selective channel measurements between sub-6 GHz and mmWave bands and we provide the corresponding measurement dataset. We outline in detail practical setup guidelines for ensuring the repeatability and the controllability of the experiments. After that, we describe the measurement campaign that has been conducted for creating the dataset. Finally, we present two illustrative ML use-cases for our dataset, namely CIR forecasting with recurrent neural networks and synthetic CTF generation with generative adversarial networks, and we suggest future exploratory research directions. Overall, our dataset provides rich, dynamic channel measurements in highly diversified scenarios of particular interest for the characterization of 5G private industrial

networks. This enables the development of innovative ML-driven methodologies on challenging real-world propagation environments. We hope that the research community will find use and inspiration in our work.

ACKNOWLEDGMENT

This work has been supported by the Austrian Research Promotion Agency (FFG) via the research project Intelligent Intersection (the national funding programme "ICT of the Future", Grant 880830) and the Christian Doppler Laboratory for Dependable Wireless Connectivity for the Society in Motion. This article is based upon work from COST Action INTERACT, CA20120, supported by COST (European Cooperation in Science and Technology).

REFERENCES

[1] F. Pasic, "Multi-band wireless channel measurements in high-mobility environment, https://dx.doi.org/10.21227/3tpp-j394, IEEE Dataport," 2022.

[2] J. Joo, M. C. Park, D. S. Han, and V. Pejovic, "Deep learning-based channel prediction in realistic vehicular communications," *IEEE Access*, vol. 7, pp. 27846–27858, 2019.

[3] C. Luo, J. Ji, Q. Wang, X. Chen, and P. Li, "Channel state information prediction for 5G wireless communications: A deep learning approach," *IEEE Transactions on Network Science and Engineering*, vol. 7, no. 1, pp. 227–236, 2020.

[4] Y. Teng, M. Liu, and M. Song, "Effect of outdated csi on handover decisions in dense networks," *IEEE Communications Letters*, vol. 21, no. 10, pp. 2238–2241, 2017.

[5] J. Connor, R. Martin, and L. Atlas, "Recurrent neural networks and robust time series prediction," *IEEE Transactions on Neural Networks*, vol. 5, no. 2, pp. 240–254, 1994.

[6] W. Jiang and H. D. Schotten, "Deep learning for fading channel prediction," *IEEE Open Journal of the Communications Society*, vol. 1, pp. 320–332, 2020.

[7] F. Pasic, S. Pratschner, R. Langwieser, D. Schützenhöfer, E. Jirousek, H. Groll, S. Caban, and M. Rupp, "Sub 6 GHz versus mmWave Measurements in a Controlled High-Mobility Environment," in *25th International ITG Workshop on Smart Antennas (WSA 2021)*, pp. 1–5, 2021. in press.

[8] F. Pasic, D. Schützenhöfer, E. Jirousek, R. Langwieser, H. Groll, S. Pratschner, S. Caban, S. Schwarz, and M. Rupp, "Comparison of Sub 6 GHz and mmWave Wireless Channel Measurements at High Speeds," in *16th European Conference on Antennas and Propagation (EuCAP 2022)*, pp. 1–5, 2022.

[9] S. Caban, J. Rodas, and J. A. García-Naya, "A methodology for repeatable, off-line, closed-loop wireless communication system measurements at very high velocities of up to 560 km/h," in *2011 IEEE International Instrumentation and Measurement Technology Conference*, 2011.

[10] M. Hofer, D. Löschenbrand, J. Blumenstein, H. Groll, S. Zelenbaba, B. Rainer, L. Bernadó, J. Vychodil, T. Mikulasek, E. Zöchmann, *et al.*, "Wireless Vehicular Multiband Measurements in Centimeterwave and Millimeterwave Bands," in *2021 IEEE 32nd Annual International Symposium on Personal, Indoor and Mobile Radio Communications (PIMRC)*, pp. 836–841, IEEE, 2021.

[11] V. Paliwal and I. Lambadaris, "Cell Search Procedures in LTE Systems," *Dept. Syst. Comput. Eng. Carleton Univ. Ottawa, ON, Canada, K1S 5B6*, pp. 1–6, 2005.

[12] B.-J. Choi, E.-L. Kuan, and L. Hanzo, "Crest-factor study of MC-CDMA and OFDM," in *50th Vehicular Technology Conference*, vol. 1, 1999.

[13] Y. Gal and Z. Ghahramani, "A theoretically grounded application of dropout in recurrent neural networks," in *Advances in Neural Information Processing Systems* (D. Lee, M. Sugiyama, U. Luxburg, I. Guyon, and R. Garnett, eds.), vol. 29, Curran Associates, Inc., 2016.

[14] B. Lim, S. O. Arık, N. Loeff, and T. Pfister, "Temporal fusion transformers for interpretable multi-horizon time series forecasting," *International Journal of Forecasting*, vol. 37, no. 4, pp. 1748–1764, 2021.

[15] A. Radford, L. Metz, and S. Chintala, "Unsupervised representation learning with deep convolutional generative adversarial networks," in *4th International Conference on Learning Representations, ICLR 2016, San Juan, Puerto Rico, May 2-4, 2016, Conference Track Proceedings* (Y. Bengio and Y. LeCun, eds.), 2016.

Faruk Pasic (Graduate Student Member, IEEE) received the Dipl.-Ing. degree (M.Sc. equivalent) from TU Wien, Austria, in 2021. He is currently pursuing the Ph.D. degree in telecommunications engineering with the Institute of Telecommunications, TU Wien. His main focus is on 5G vehicular-to-everything (V2X) communications.

Nicola Di Cicco (Graduate Student Member, IEEE) is currently working towards the Ph.D. degree with the Department of Electronic, Information, and Bioengineering, Politecnico di Milano, Milan, Italy. His research interests include deep learning and reinforcement learning for network optimization and automation.

Marco Skocaj (Graduate Student Member, IEEE) is currently working towards the Ph.D. degree with the Department of Electronic, Information and Electrical Engineering at the University of Bologna and WiLab, CNIT. He is chair of HA1 (Datasets) working group in COST action 20120 INTERACT. His research interests include Radio Resource Management, Machine Learning, Autonomous Networks and Optimization.

Massimo Tornatore (Fellow, IEEE) is currently an Associate Professor with the Department of Electronics, Information, and Bioengineering, Politecnico di Milano. His research interests include performance evaluation, optimization and design of communication networks, network virtualization, network reliability, and machine learning application for network management.

Stefan Schwarz (Senior Member, IEEE) received the Dr. techn. degree (Ph.D. equivalent) in telecommunications engineering from TU Wien, Austria, in 2013. Since 2021, he is as an Associate Professor with the Institute of Telecommunications, TU Wien, where he also heads the Christian Doppler Laboratory for Dependable Wireless Connectivity. His research interests include wireless communications, signal processing, channel modeling and machine learning. He is an Associate Editor of IEEE Access, IEEE Communications Letters and EURASIP JWCN.

Christoph F. Mecklenbräuker (Senior Member, IEEE) received the Dipl.-(Ing.) degree (Hons.) in electrical engineering from TU Wien, Vienna, Austria, in 1992, and the Dr.-(Ing.) degree (Hons.) from Ruhr-Universität Bochum, Bochum, Germany, in 1998. Since 2006, he has been a Full Professor with the Institute of Telecommunications, TU Wien. His current research interests include 5G and 6G radio interfaces and antennas and propagation.

Vittorio Degli-Esposti (Senior Member, IEEE) is currently Associate Professor with the Department of Electrical Engineering of the University of Bologna and previously Director of Research at Polaris Wireless Inc., USA, in 2015-2016. He is Chair of the Propagation Working Group of the European Association on Antennas and Propagation (EurAAP) He is author or co-author of over 150 peer-reviewed technical papers and co-inventor of 7 international patents in the fields of applied electromagnetics, radio propagation and wireless systems.